AD-A132 109 PONDEROMOTIVE EFFECTS IN NONNEUTRAL PLASMAS(U) 1/1
CALIFORNIA UNIV LOS ANGELES CENTER FOR PLASMA PHYSICS
AND FUSION ENGINEERING B M LAMB ET AL. MAY 83 PPG-711
UNCLASSIFIED N00014-76-C-0476 F/G 20/9 NL

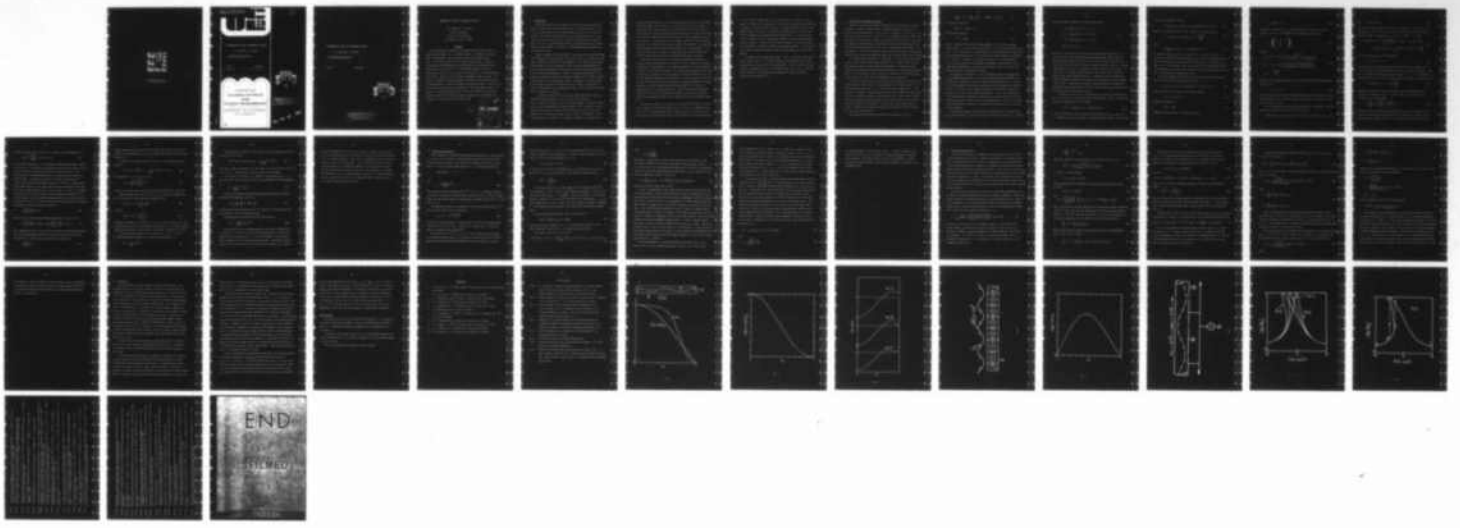

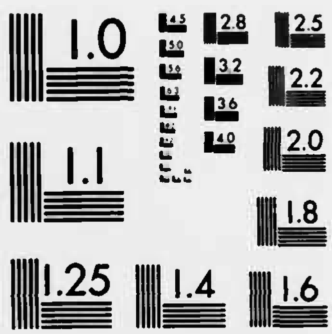

PONDEROMOTIVE EFFECTS IN NONNEUTRAL PLASMAS

B. M. Lamb and G. J. Morales

Contract N00014-76-C-0476

PPG-711 May 1983

CENTER FOR
PLASMA PHYSICS
AND
FUSION ENGINEERING

UNIVERSITY OF CALIFORNIA
LOS ANGELES

PONDEROMOTIVE EFFECTS IN NONNEUTRAL PLASMAS

B. M. Lamb and G. J. Morales

Contract N00014-76-C-0476

PPG-711 May 1983

PONDEROMOTIVE EFFECTS IN NONNEUTRAL PLASMAS

B. M. Lamb and G. J. Morales

Physics Department

University of California

Los Angeles, California 90024

ABSTRACT

This investigation considers the ponderomotive effects which arise in a single species plasma, i.e., a nonneutral plasma. The important difference from a neutral plasma is that quasi-neutral density cavities given by $\delta n/n_o \simeq -|\underset{\sim}{E}|^2/16\pi n_o T$ cannot arise in a single species plasma. Instead, it is found that the ponderomotive force is balanced by self-consistent space charge fields, and results in $\delta n \simeq \nabla^2|E_{\parallel}|^2/16\pi m\omega^2$, where ω is the frequency and $E_{\parallel}$ refers to the wave electric field parallel to the confining magnetic field. In addition to the density rearrangement, the zero order $\underset{\sim}{E} \times \underset{\sim}{B}$ rotation is modified. The self-consistent nonlinear state has been found for a large amplitude $\ell = 0$ axially standing Gould-Trivelpiece wave. The linear dispersion relation is modified by the presence of the large amplitude wave, and results in a nonlinear frequency shift. This shift produces an interesting hysteresis effect in the nonlinear resonant response of the plasma when the frequency of the external driver is swept slowly.

I. INTRODUCTION

Nonlinear wave effects in plasmas fall into two broad categories: wave-particle interactions and fluid nonlinearities. For waves whose phase velocities are much larger than the average thermal velocities of all particle species, the wave-particle interaction plays an insignificant role. In such systems the fluid nonlinearities are primarily responsible for the modification of the zero order plasma equilibrium as the wave amplitude is increased beyond the linear regime. The subject of the present analytical study falls into the latter class.

Among the numerous fluid nonlinearities associated with a large amplitude, high frequency, electrostatic wave, there are two effects of overwhelming importance: parametric instabilities and ponderomotive force density modifications. In conventional neutral plasmas both of these can appear simultaneously and lead to interesting physical effects which have been extensively investigated theoretically and experimentally. However, in single species plasmas, i.e., nonneutral plasmas, the parametric instability channel is not readily available because there is only a single mass present. Consequently, in these systems it is expected that the first nonlinear effect to appear is modification of the zero order density by the ponderomotive force. This is the specific issue that is considered in this work.

It is widely accepted[1,2] that in neutral plasmas the density changes δn produced by the ponderomotive force are given by the expression $\delta n/n_o = -|\underset{\sim}{E}|^2/16\pi n_o T$, where n_o is the zero order density, T the plasma temperature, and $|\underset{\sim}{E}|$ the amplitude of the high frequency field. Physically, the end result can be viewed as a pressure balance between the wave and the plasma. However, in the calculation leading to such a result, the existence of a neutralizing species is essential. The sequence of events can be understood by

the following time ordering. First the high frequency field acts on the lighter species and pushes these particles out of the regions where $|\underset{\sim}{E}|$ is maximum. An intermediate space charge separation results from the relative displacement of the two species. Finally, the heavier species responds to the space charge field and follows the lighter species, thus resulting in a density depression which is overall neutral. From this picture it is apparent that when the second species is absent, the resulting density change is significantly modified. In particular, balancing kinetic pressure against field pressure is no longer possible. It is the aim of this study to provide a relevant description of the ponderomotive effect when the neutralization due to a second charge species is absent.

Technically, the difficulty in calculating the ponderomotive effect in a nonneutral plasma arises because of the need to satisfy a global self-consistent equilibrium in finite geometry. In a nonneutral system once a charge separation is induced, all zero order quantities, e.g., density, space potential, and rotation, are modified. In addition, the strong symmetry requirements imposed by the zero order confinement scheme must be incorporated. To obtain a concrete result that includes all these effects, the present study isolates the ponderomotive changes produced by an axially standing Gould-Trivelpiece mode[3,4] in a nonneutral plasma column that is strongly magnetized. Aside from defining the prototype problem in this class, the situation is realizable in the various nonneutral plasma devices developed recently[5,6] which exhibit excellent confinement properties.

The principal result of this study is that a fully self-consistent ponderomotive change can be obtained analytically for the case of an azimuthally symmetric ($\ell = 0$) Gould-Trivelpiece mode. Near the center of the column the density change is found to be proportional to the Laplacian of the field amplitude,

i.e., $\delta n \propto \nabla^2 |\underset{\sim}{E}|^2$ instead of the conventional result $\delta n \propto -|\underset{\sim}{E}|^2$ for a neutral plasma. In addition, the consequences of the density change have been calculated. It produces a nonlinear frequency shift of all modes satisfying the proper wave number matching conditions. An interesting hysteresis effect is found in the resonant response of the standing Gould-Trivelpiece mode. It arises when the nonlinear frequency shift is comparable in magnitude to the collisional broadening of the mode. A similar effect has been obtained in a recent low temperature experiment[7] involving a two dimensional nonneutral plasma. It is found here that a three dimensional nonneutral plasma can also exhibit this nonlinear phenomenon.

The manuscript is organized as follows: In Sec. II we derive the ponderomotive effects due to a $\ell = 0$ axially standing Gould-Trivelpiece wave without specializing to a specific zero order equilibrium. In order to obtain concrete results we consider a rigid rotor equilibrium in Sec. III. In Sec. IV the nonlinear frequency shift produced by the ponderomotive force is presented. Conclusions are given in Sec. V.

II. DERIVATION OF PONDEROMOTIVE EFFECTS

Consider a cylindrically symmetric nonneutral plasma consisting of particles of charge q and mass m confined inside a conducting cylinder of radius a by a strong, uniform axial magnetic field $\underset{\sim}{B} = B_o \hat{z}$, as illustrated in Fig. 1(a). Cylindrical coordinates are utilized, with the z axis coinciding with the cylinder axis. For simplicity, the plasma is assumed to be infinite in axial extent. This assumption removes some interesting, but complicating, physical effects associated with the nonlinear lengthening which can occur in a finite length plasma column. An axisymmetric ($\ell = 0$) Gould-Trivelpiece standing wave is envisioned to be resonantly driven so that a steady state amplitude results due to weak collisions with neutrals.

The problem under investigation in this study is to find the nonlinear modifications of the zero order equilibrium quantities, e.g., density, space potential, and rotation, caused by a large amplitude standing wave. The effect of these changes in the equilibrium quantities upon the properties of the Gould-Trivelpiece modes is also investigated. Since the problem is periodic in the axial direction, it need only be analyzed within one wavelength of the standing wave.

The essential physics of the problem can be treated using a fluid description provided that the phase velocity is large compared to the thermal velocity. For Gould-Trivelpiece modes with $\omega < \omega_p << \Omega$ this condition is readily met. Unlike theoretical treatments of neutral plasmas which are often modeled as being infinite and uniform, nonneutral plasmas are necessarily of finite radial extent because of the resulting large self-electric fields. Due to this property one must consider a specific equilibrium configuration in order to pose a well defined problem; however, in spite of this restriction, the results obtained in the present study are of a fairly general nature.

The response of the system is described by the equation of motion,

$$\mathcal{N}\left[\frac{\partial}{\partial t}\underset{\sim}{\mathcal{V}} + \underset{\sim}{\mathcal{V}}\cdot\nabla\underset{\sim}{\mathcal{V}}\right] = -\frac{q}{m}\mathcal{N}\nabla + \Omega\mathcal{N}\underset{\sim}{\mathcal{V}}\times\hat{z} - \frac{1}{m}\nabla\mathcal{P}, \tag{1}$$

the continuity equation,

$$\frac{\partial}{\partial t}\mathcal{N} + \nabla\cdot(\mathcal{N}\underset{\sim}{\mathcal{V}}) = 0, \tag{2}$$

and Poisson's equation,

$$\nabla^2\Phi = -4\pi q\mathcal{N}, \tag{3}$$

where $\Omega \equiv qB_o/mc$ is the cyclotron frequency, $\mathcal{N}(r, z, t)$ is the total plasma density, $\underset{\sim}{\mathcal{V}}(r, z, t)$ is the fluid velocity, $\mathcal{P}(r, z, t)$ is the thermal pressure, and $\Phi(r, z, t)$ is the potential. The self-magnetic field generated by the plasma rotation has been neglected in Eq. (1) because, for the plasma parameters considered, i.e., $\omega_p{}^2 a/\Omega c << 1$ (where ω_p is the plasma frequency), it is small compared to B_o. We also assume the electromagnetic wavelength is long compared to the characteristic dimensions of the physical system, i.e., $\omega a/c << 1$, so that the quasi-electrostatic approximation is valid.

We proceed to solve Eqs. (1) - (3) by ordering according to the amplitude of the Gould-Trivelpiece wave. The linear wave quantities are considered to be a first order perturbation to the zero order equilibrium quantities. In second order the ponderomotive force appears through the time independent (dc) component of the $\underset{\sim}{\mathcal{V}}\cdot\nabla\underset{\sim}{\mathcal{V}}$ term. At this stage we consider only the dc second order modifications to the zero order equilibrium quantities. In Sec. IV we feedback the second order modified equilibrium quantities into a nonlinear dispersion relation to obtain a nonlinear frequency shift of the standing wave. The effect of second order contributions at harmonics of the linear wave frequency are not considered in this manuscript.

The electric potential, density, velocity, and pressure are separated into three terms consisting of zero order equilibrium, linear response, and dc quadratic

nonlinear changes produced by the large amplitude wave:

$$\begin{aligned}
\Phi &= \phi_o + \tfrac{1}{2}[\tilde{\phi}\ \exp(-i\omega t) + \text{c.c.}] + \delta\phi, \\
\mathcal{N} &= n_o + \tfrac{1}{2}[\tilde{n}\ \exp(-i\omega t) + \text{c.c.}] + \delta n, \\
\mathcal{V} &= V_o\hat{\theta} + \tfrac{1}{2}[\tilde{\underset{\sim}{v}}\ \exp(-i\omega t) + \text{c.c.}] + \delta\underset{\sim}{v}, \\
\nabla\mathcal{P} &= T\ \nabla\ (n_o + \delta n),
\end{aligned} \tag{4}$$

where $\phi_o(r)$, $n_o(r)$, and $V_o(r)$ are zero order equilibrium quantities, $\tilde{\phi}\ (r,z)$, $\tilde{n}(r,z)$, and $\tilde{\underset{\sim}{v}}(r,z)$ are complex amplitudes representing the linear response to the high frequency wave at frequency ω, and $\delta\phi(r,z)$, $\delta n(r,z)$, and $\delta\underset{\sim}{v}(r,z)$ are the steady state self-consistent nonlinear changes produced by the wave. Constant temperature is used for the dc quantities because, as we later find in Sec. III, in the bulk of the plasma column temperature plays a small role in the force balance against the ponderomotive force. In addition, no explicit usage of a collision frequency is made at this stage; the wave amplitude is simply assumed to be constant. Temperature corrections to the wave quantities are neglected because for Gould-Trivelpiece waves, both the phase velocity and the group velocity are much greater than the thermal velocity.

An equation for the zero order equilibrium is obtained by substituting from Eq. (4) into Eqs. (1) - (3) and setting the wave amplitude to zero. For this condition the r component of Eq. (1) becomes

$$-\frac{1}{r}V_o^{\,2} = -\frac{q}{m}\frac{\partial}{\partial r}\ \phi_o + \Omega\ V_o - \frac{T}{m}\frac{\partial}{\partial r}\ln(n_o/n_p), \tag{5}$$

in which the density has been normalized to the density on axis $n_p \equiv n_o(r = 0)$.

Operating on Eq. (5) with $\frac{1}{r}\frac{\partial}{\partial r}\,r$ and using Poisson's equation to eliminate ϕ_o

yields the differential equation

$$\lambda_D^2 \frac{1}{r}\frac{\partial}{\partial r} r \frac{\partial}{\partial r} \ln(n_o/n_p) - n_o/n_p = \frac{1}{\omega_p^2}\frac{1}{r}\frac{\partial}{\partial r}[V_o(\Omega r + V_o)], \tag{6}$$

where $\omega_p^2 \equiv 4\pi n_p q^2/m$ and $\lambda_D^2 = 1/K_D^2 \equiv T/4\pi n_p q^2$. Using the scaling

$$\rho \equiv r/\lambda_D,\ N(\rho) \equiv n_o(r/\lambda_D)/n_p,\ A(\rho) \equiv \frac{V_o(r/\lambda_D)}{\sqrt{T/m}}, \tag{7}$$

gives

$$\frac{1}{\rho}\frac{\partial}{\partial\rho}\left[\rho\frac{\partial}{\partial\rho}\ \ell n\ N\right] - N = \frac{1}{\rho}\frac{\partial}{\partial\rho}[A(\Omega\rho/\omega_p + A)]. \tag{8}$$

The boundary conditions for Eq. (8) are $N(\rho = 0) = 1$ and $N(\rho = a/\lambda_D) = 0$. Equation (8) may be satisfied by assuming a given form for the density profile $N(\rho)$ and solving for the resulting scaled velocity $A(\rho)$, or conversely as is done in Sec. III, by taking a rigid rotor velocity profile and solving for $N(\rho)$. The requirement that N must vanish at the wall places constraints upon the rotation velocities which are physically allowed.

The linear response quantities $\tilde{\phi}(r,z)$, $\tilde{n}(r,z)$, and $\underset{\sim}{\tilde{v}}(r,z)$ are separated from Eqs. (1)-(3) giving the equation of motion,

$$-i\omega \underset{\sim}{\tilde{v}} - \frac{2}{r} V_o \tilde{v}_\theta \hat{r} + \frac{1}{r}\tilde{v}_r \frac{\partial}{\partial r}(rV_o)\hat{\theta} = -\frac{q}{m}\nabla\tilde{\phi} + \Omega \underset{\sim}{\tilde{v}} \times \hat{z}, \tag{9}$$

where $\hat{r}$ and $\hat{\theta}$ are unit vectors, the continuity equation,

$$-i\omega \tilde{n} + \nabla \cdot (n_o \underset{\sim}{\tilde{v}}) = 0, \tag{10}$$

and Poisson's equation,

$$\nabla^2 \tilde{\phi} = -4\pi q\tilde{n}. \tag{11}$$

Equation (9) is solved for $\underset{\sim}{\tilde{v}}$ in terms of $\tilde{\phi}$ giving

$$\underset{\sim}{v} = \frac{i\omega}{qn_o} \underset{\sim}{\chi} \cdot \nabla \phi_o, \tag{12}$$

in which the susceptibility $\underset{\sim}{\chi}$ is defined in terms of the dielectric tensor through $\underset{\sim}{\varepsilon} = \underset{\sim}{1} + 4\pi\underset{\sim}{\chi}$. The components of the dielectric tensor are

$$\underset{\sim}{\varepsilon} = \begin{pmatrix} \varepsilon_{rr} & \varepsilon_{r\theta} & 0 \\ \varepsilon_{\theta r} & \varepsilon_{\theta\theta} & 0 \\ 0 & 0 & \varepsilon_{zz} \end{pmatrix}, \tag{13}$$

in which

$$\varepsilon_{rr} = \varepsilon_{\theta\theta} = 1 - \frac{\omega_p^2(r)}{\omega^2 - [\Omega + 2V_o(r)/r][\Omega + 1/r\ \partial/\partial r(rV_o(r))]},$$

$$\varepsilon_{r\theta} = -\varepsilon_{\theta r} = \frac{-i\ [\Omega + 1/r\ \partial/\partial r\ (rV_o(r))]\omega_p^2(r)/\omega}{\omega^2 - [\Omega + 2V_o(r)/r][\Omega + 1/r\ \partial/\partial r(rV_o(r))]}, \tag{14}$$

$$\varepsilon_{zz} = 1 - \frac{\omega_p^2(r)}{\omega^2}.$$

Equation (12) is combined with Eqs. (10) and (11) giving a partial differential equation for $\tilde{\phi}$

$$\nabla \cdot \underset{\sim}{\varepsilon} \cdot \nabla \tilde{\phi} = 0. \tag{15}$$

The linear normal modes of the nonneutral plasma system are obtained by solving Eq. (15) subject to the boundary condition that $\tilde{\phi}(r=a,z) = 0$ and the condition that $\tilde{\phi}$ is finite on axis.

The time averaged (dc) nonlinear quantities which are quadratic in the wave amplitude are separated from Eqs. (1) and (3) giving

$$-\frac{2m}{r} V_o\ \delta V_\theta\ \hat{r} + q\ \nabla\ \delta\phi - m\Omega\ \delta V_\theta\ \hat{r} + T\ \nabla\ \delta n/n_o = -\ m/2\ \mathrm{Re}(\underset{\sim}{\tilde{v}}^* \cdot \nabla\ \underset{\sim}{\tilde{v}}), \tag{16}$$

and $$\nabla^2 \delta\phi = -4\pi q\, \delta n. \tag{17}$$

Notice that Eq. (16) contains the driving term $-m/2\ \mathrm{Re}(\tilde{v}^* \cdot \nabla \tilde{v})$, which is the ponderomotive force of the wave. The factor of one-half results from taking the time average. Substituting Eq. (12) into $-m/2\ \mathrm{Re}(\tilde{v}^* \cdot \nabla \tilde{v})$ gives

$$-m/2\ \mathrm{Re}(\tilde{v}^* \cdot \nabla \tilde{v}) = -\frac{4\pi^2 q^2 \omega^2}{m\omega_p^4}\left\{\hat{z}\left[\chi_{zz}^2\ \frac{\partial}{\partial z}\,|\tilde{E}_z|^2 + \chi_{rr}\chi_{zz}\,\frac{\partial}{\partial z}\,|\tilde{E}_r|^2\right]\right. \tag{18}$$
$$\left. + \hat{r}\left[\chi_{rr}^2\,\frac{\partial}{\partial r}\,|\tilde{E}_r|^2 + \chi_{rr}\chi_{zz}\,\frac{\partial}{\partial r}\,|\tilde{E}_z|^2 - \frac{2}{r}\,|\chi_{r\theta}|^2\,|\tilde{E}_r|^2\right]\right\},$$

in which $\tilde{E}_r$ and $\tilde{E}_z$ have been defined using

$$\tilde{E}_r\,\hat{r} + \tilde{E}_z\,\hat{z} = -\nabla\tilde{\phi}, \tag{19}$$

and derivatives of χ/ω_p^2 have been neglected since they are of higher order in ω_p^2/Ω^2, which is assumed throughout this work to be a small correction. Since we are considering a strongly magnetized plasma with $\omega < \omega_p << \Omega$, the general ponderomotive force in Eq. (18) is approximated as the lowest order term in ω_p^2/Ω^2,

$$-\,m/2\ \mathrm{Re}(\tilde{v}^* \cdot \nabla \tilde{v}) \simeq -\,\hat{z}\,\frac{\partial}{\partial z}\,\frac{q^2|\tilde{E}_z|^2}{4m\omega^2}\ , \tag{20}$$

which physically means that only the component of the ponderomotive force parallel to the magnetic field is retained. With this approximation the z component of Eq. (16) becomes

$$\frac{\partial}{\partial z}\left[\frac{q}{m}\,\delta\phi + \frac{q^2|\tilde{E}_z|^2}{4m^2\omega^2} + \frac{T}{m}\,\frac{\delta n}{n_o}\right] = 0, \tag{21}$$

which states that, in the strongly magnetized limit, the self-consistent electrostatic force, modified pressure force, and ponderomotive force must be balanced along each magnetic field line. This equation implies that the quantity

within the brackets may be set equal to a function f(r), independent of z,

$$\frac{q}{m}\,\delta\phi + \frac{q^2|\tilde{E}_z|^2}{4m^2\omega^2} + \frac{T}{m}\,\delta n/n_o = f(r). \tag{22}$$

Any f(r) which vanishes at r = a represents an allowable equilibrium. However in the context of a deterministic experiment, one must find the appropriate f(r) which corresponds to the equilibrium which the system evolves to as the wave amplitude is increased adiabatically in a well defined zero order non-neutral plasma. Two important constraints are used in determining f(r). Particle number should be conserved because an $\ell = 0$ wave in a strongly magnetized plasma should not cause radial plasma transport, and because in our axially infinite model particles may not be lost axially. Of course, in an experiment particles are axially confined by large electrostatic barriers.[5,6] The second constraint is that canonical angular momentum must be conserved because the excitation of an $\ell = 0$ wave does not apply an external torque to the system. The statement of particle number conservation is

$$\frac{\lambda}{2}\int_{-\lambda/4}^{+\lambda/4} dz \int_o^a rdr\ \delta n = 0, \tag{23}$$

and the conservation of canonical angular momentum P_θ to order ω_p^2/Ω^2 is

$$\frac{\lambda}{2}\int_{-\lambda/4}^{+\lambda/4} dz \int_o^a 2\pi rdr\ qrA_\theta\delta n/c = \frac{1}{2}m\Omega\,\frac{\lambda}{2}\int_{-\lambda/4}^{+\lambda/4} dz \int_o^a 2\pi rdr\ r^2\delta n = 0. \tag{24}$$

The z integrations in Eqs. (23) and (24) are performed over one-half wavelength λ of the axial standing wave because δn is expected to have axial variations with period $\lambda/2$. Both the above conditions can be satisfied if

$$\frac{\lambda}{2}\int_{-\lambda/4}^{+\lambda/4} \delta n\ dz = 0, \tag{25}$$

which means physically that plasma is rearranged along each field line in response to the ponderomotive force of the standing wave without transport across field lines.

We obtain f(r) by operating with ∇^2 on Eq. (22), substituting Poisson's equation,

$$\frac{T}{m} \nabla^2 \delta n/n_o - \frac{4\pi q^2}{m} \delta n = - \frac{q^2}{4m^2\omega^2} \nabla^2 |\tilde{E}_z|^2 + \nabla^2 f(r), \tag{26}$$

and integrating in z from $-\lambda/4$ to $+\lambda/4$:

$$f(r) = \frac{q^2}{4m^2\omega^2} \frac{\lambda}{2} \int_{-\lambda/4}^{+\lambda/4} |\tilde{E}_z|^2 \, dz, \tag{27}$$

in which use has been made of the sinusoidal axial variation of δn and $|\tilde{E}_z|^2$.

Having determined the correct choice for f(r), Eq. (22) is combined with Eq. (17), giving a partial differential equation for $\delta\phi$,

$$\lambda_D^2 \nabla^2 \delta\phi - \delta\phi = \frac{q}{4m\omega^2} \delta|\tilde{E}_z|^2, \tag{28}$$

in which

$$\delta|\tilde{E}_z|^2 \equiv |\tilde{E}_z|^2 - \frac{\lambda}{2}\int_{-\lambda/4}^{+\lambda/4} |E_z|^2 \, dz, \tag{29}$$

and having the boundary condition $\delta\phi(r = a, z) = 0$. One may interpret Eq. (28) by saying that the term $-1/4\pi\lambda_D^2(q/4m\omega^2)\ \delta|\tilde{E}_z|^2$ represents an effective nonlinear charge density induced by the wave which is then Debye shielded by the plasma.

In the appropriate plasma limit for which $K_D a >> 1$, the $\nabla^2\ \delta\phi$ term of Eq. (28) becomes small compared to $\delta\phi$ and one may approximate $\delta\phi$ as

$$\delta\phi \simeq - \frac{q}{4m\omega^2} \delta|\tilde{E}_z|^2. \tag{30}$$

Substituting Eq. (27) into Eq. (26) results in the following partial differential equation for $\delta n/n_o$

$$\lambda_D^2 \nabla^2 \delta n/n_o - N(r/\lambda_D)\, \delta n/n_o = - \frac{1}{16\pi n_p m\omega^2} \nabla^2 \delta|\tilde{E}_z|^2. \qquad (31)$$

The correct boundary condition for Eq. (31) when $T \neq 0$ is seen from Eq. (21) to be $\delta n/n_o \to 0$ as $r \to a$ because both $\delta\phi$ and $\tilde{E}_z$ are zero on the boundary.

In the bulk of the plasma, i.e., outside of a sheath region near $r = a$, the first term of Eq. (31) goes as λ_D^2/a^2; in this region δn may be approximated as

$$\delta n = \frac{1}{16\pi m\omega^2} \nabla^2 \delta|\tilde{E}_z|^2. \qquad (32)$$

Finally, the azimuthal nonlinear velocity modification δV_θ is obtained from the radial component of Eq. (16),

$$\delta V_\theta = \frac{1}{\Omega^*} \frac{\partial}{\partial r} \left[\frac{q}{m} \delta\phi + \frac{T}{m} \delta n/n_o\right], \qquad (33)$$

in which we have used the definition $\Omega^* \equiv \Omega + 2V_o(r)/r$ of the effective cyclotron frequency in the rotating plasma frame.

Substituting Eqs. (22) and (27) into Eq. (33) results in

$$\delta V_\theta = - \frac{q^2}{4m^2\omega^2\Omega^*} \frac{\partial}{\partial r} \delta|\tilde{E}_z|^2. \qquad (34)$$

We note that δV_θ does not depend explicitly on the plasma temperature T, even though it is the sum of the $\underset{\sim}{E} \times \underset{\sim}{B}$ drift resulting from $- q \nabla \delta\phi$ and the diamagnetic drift resulting from $- T \nabla \delta n$ with the magnetic field being the effective magnetic field in the rotating plasma frame. The physical interpretation of Eq. (21) is that the electric force and the pressure force combine to

balance the ponderomotive force in the z direction. However, since the electric force and pressure force are gradients of scalars, while the ponderomotive force in a magnetized plasma is not, there is an unbalanced force in the radial direction given by $q^2/4m\omega^2\ \hat{r}\frac{\partial}{\partial r}\ |\tilde{E}_z|^2$. δV_θ is just the drift resulting from this force and thus is temperature independent. Note that since this drift does not depend upon the specific nature of the force balance, i.e., whether the ponderomotive force is balanced against pressure as in a neutral plasma or against electrostatic forces as in a nonneutral plasma, it must also exist in a strongly magnetized neutral plasma.

III. Rigid Rotor Equilibrium

Most treatments of nonneutral plasma equilibria specialize to rigid rotors,[8,9] i.e., $V_o(r) = \omega_R r$ such that the plasma executes a bulk rotation about its axis. In this section we consider a rigid rotor with a density profile which is flat from r = 0 to within several Debye lengths of r = a. Equation (8) reduces to

$$\frac{1}{\rho}\frac{\partial}{\partial\rho}\rho\frac{\partial}{\partial\rho}\ell n\, N - N + 1 = \gamma, \tag{35}$$

with

$$\gamma \equiv -\frac{2\omega_R(\omega_R + \Omega)}{\omega_p^2} - 1. \tag{36}$$

This equation has been previously solved.[10,11] For $\gamma \simeq 0$ it possesses solutions for which N is uniform for many Debye radii and smoothly falls to zero in a sheath region of several Debye lengths in radial extent, as shown in Fig. 1(b) for $\gamma = .004$ and $a = 10\ \lambda_D$.

The approximate values of ω_R allowed by Eq. (35) are found by setting $\gamma = 0$ in Eq. (36) and solving for ω_R. This gives

$$\omega_R = -\frac{\Omega}{2}\left(1 \pm \sqrt{1 - 2\omega_p^2/\Omega^2}\right) \tag{37}$$

The slow rotational mode given by the minus sign in (37), in the strongly magnetized limit of $\omega_p^2 << \Omega^2$, is $\omega_R \simeq -\omega_p^2/2\Omega$, which is simply the $\underset{\sim}{E} \times \underset{\sim}{B}$ velocity due to the associated space charge field.

The solutions of Eq. (15) for $\omega < \omega_p << \Omega$ are the Gould-Trivelpiece modes of a nonneutral plasma column. For the purpose of studying these waves we shall neglect the sheath region by approximating the zero order density as constant.

Since $\tilde{\phi}$ must vanish at r = a, this is a good approximation if the sheath region is small compared to the column radius a. A constant density solution of Eq. (15) with $\tilde{\phi} = 0$ on the conducting boundary at r = a is

$$\tilde{\phi} = E_o/k\ J_o(\chi_{on}\ r/a)\ \sin kz, \tag{38}$$

in which E_o is an electric field magnitude, J_o is a Bessel function, and χ_{on} is the n^{th} zero of the J_o Bessel function. The dispersion relation becomes

$$k^2a^2 = -\frac{\chi_{on}^2}{1-\omega_p^2/\omega^2}\ . \tag{39}$$

If the phase velocity ω/k is large compared to the thermal velocity $\sqrt{T/m}$ or equivalently if $k^2\lambda_D^2 << \omega^2/\omega_p^2$, Landau damping is negligible. Using Eq. (39) this requires that $\omega^2/\omega_p^2 << 1 - \chi_{on}^2/K_D^2a^2$. Recalling that $K_D^2a^2 >> 1$ for typical nonneutral plasmas,[5,6] we see that in the regime we are considering, $\omega < \omega_p << \Omega$, weakly damped waves can exist. Thus by externally driving the plasma at frequency ω, the excited Gould-Trivelpiece waves can become steady state axially standing waves.

Using the defining relation for $\delta|\tilde{E}_z|^2$, Eq. (29), gives

$$\delta|\tilde{E}_z|^2 = \frac{1}{2}\ E_o^2\ J_o^2\ (\chi_{on}\ r/a)\ \cos 2kz. \tag{40}$$

For the first radial eigenmode, i.e., n = 1, this quantity decreases in the radial direction as shown in Fig. 2, and varies axially as cos2kz.

Inserting Eq. (40) into Eq. (31) gives

$$\lambda_D^2\ \nabla^2(\delta n/n_o) - (\delta n/n_o) = -\frac{n_s}{2n_p}\frac{a^2}{\chi_{on}^2}\nabla^2\left[J_o^2(\chi_{on}\ r/a)\ \cos 2kz\right] - (1 - n_o/n_p)\ \delta n/n_o, \tag{41}$$

with

$$n_s \equiv \frac{E_o^2 \chi_{on}^2}{16\pi a^2 m\omega^2}. \tag{42}$$

The term $(1 - n_o/n_p)\ \delta n/n_o$ is placed on the right side of the equation so that an iterative solution for $\delta n/n_o$ may be obtained by using the Green's function for the left side. Two finite temperature solutions for δn obtained in this manner using the correct finite temperature zero order profile, $n_o(r)$, are shown in Fig. 3. The zero temperature solution of Eq. (32) is

$$\delta n = n_s\left[J_1^2(\chi_{on}\ r/a) - (1 + 2k^2a^2/\chi_{on}^2)\ J_o^2\ (\chi_{on}\ r/a)\right]\cos 2kz, \tag{43}$$

and is plotted as the upper curve in Fig. 3.

On axis, the ponderomotive force expels particles from the regions where $|\tilde{E}_z|$ is large and causes a density increase where $|\tilde{E}_z|$ is small as illustrated in Fig. 4. The electrostatic field arising from this density rearrangement balances the ponderomotive force. Since this effect is two dimensional, the charge bunching along the axis produces a fringing electric field which influences the force balance at outer radii. Since $\delta|\tilde{E}_z|^2$ decreases monotonically with r, a radius is reached at which the fringing electric field due to charges at inner radii is greater than the field required to balance the ponderomotive force at that radial position. From this radius outward, the density rearrangement changes sign, i.e., density increases axially where $|\tilde{E}_z|$ is large and a density depletion occurs where $|\tilde{E}_z|$ is small. This effect is seen in Fig. 3, and is in direct contrast to the situation in a neutral plasma in which this fringing effect is not present; in neutral plasmas the ponderomotive force is balanced against plasma pressure and Poisson's equation is never utilized because quasi-neutrality is satisfied.

The radial dependence of the nonlinear density modification $\delta n(z = 0)$ is shown in Fig. 3 for zero temperature, $K_D a = 25$, and $K_D a = 10$; δn has the same

axial dependence as $\delta|\tilde{E}_z|^2$ of cos2kz. At z = 0, $\delta|\tilde{E}_z|^2$ has a maximum and thus δn is negative on axis and positive at outer radii as shown in Fig. 3. At an axial position where $\delta|\tilde{E}_z|^2$ is negative, δn becomes positive on axis and negative at outer radii. The primary effect of finite plasma temperature occurs in the sheath within several Debye lengths of r = a. For zero temperature the density drops discontinuously to zero at r = a, but for finite temperature the density drops smoothly to zero. Finite temperature also gives rise to a slight reduction in the magnitude of δn near the column axis.

It can be concluded that, for typical nonneutral plasma parameters, the ponderomotive force, $-\hat{z}\frac{\partial}{\partial z}\frac{q^2}{4m\omega^2}\delta|\tilde{E}_z|^2$, is balanced against an axial electrostatic force, $-\hat{z}\frac{\partial}{\partial z}q\delta\phi$, rather than the much smaller pressure force. Pressure forces only play a significant role in the sheath region (the outer several Debye radii). The associated density modification δn is obtained from $\delta\phi$ through Poisson's equation; the force balance equation is of little use because of the near exact cancellation between the ponderomotive force and the electrostatic force. The modified electrostatic potential $\delta\phi$ has a radial electric field $-\hat{r}\frac{\partial}{\partial r}\delta\phi$ associated with it which is not balanced against the ponderomotive force since the radial component of the ponderomotive force is negligibly small in the strongly magnetized limit. This radial electric field changes the rotational velocity of the plasma. Substituting Eq. (40) into Eq. (34) gives this nonlinear velocity modification δV_θ,

$$\delta V_\theta = V_s\, J_o(\chi_{on}\, r/a)\, J_1(\chi_{on}\, r/a)\, \cos 2kz, \tag{44}$$

with

$$V_s \equiv \frac{q^2 E_o^2}{4m^2\omega^2\Omega^*}\,\frac{\chi_{on}}{a}. \tag{45}$$

The radial dependence of δV_θ is shown in Fig. 5. A shear is produced in the velocity profile, but we do not examine any possible instabilities resulting from this shear. Since both δn and δV_θ have an axial dependence of cos2kz, the canonical angular momentum is on the average unchanged, as expected for an axisymmetric wave.

IV. Nonlinear Frequency Shift

The density rearrangement δn produced by the ponderomotive force of a large amplitude standing wave can cause a nonlinear modification in the dispersion relation of the modes supported by the plasma. In addition to the self-modification of the large amplitude mode, all modes, e.g., plasma noise, satisfying proper wave number matching conditions are nonlinearly modified. In this section the nonlinear resonant frequency shift of Gould-Trivelpiece modes resulting from externally driving the plasma at frequency ω is found. For simplicity, all calculations in this section are performed for zero temperature and an initially flat density profile, since it was demonstrated in Sec. III that thermal effects are small for typical nonneutral plasma parameters.

An idealized antenna that excites waves with a given axial wavelength can be obtained by cutting the conducting cylinder into sections of length $\lambda/2$ and driving adjacent sections with alternating polarities, as illustrated in Fig. 6. Waves of axial wavenumber $k = 2\pi/\lambda$ and odd harmonics thereof are excited in the nonneutral plasma column. The linear plasma response is given by the superposition of modes which satisfy the proper boundary condition at $r = a$,

$$\tilde{\phi} = \sum_{j=o}^{\infty} \frac{4V_{rf}}{\pi(2j+1)} \frac{J_o[(2j+1)(\omega_p^2/\omega^2-1)^{1/2}kr]}{J_o[(2j+1)(\omega_p^2/\omega^2-1)^{1/2}ka]} \sin[(2j+1)kz], \tag{46}$$

in which V_{rf} is the amplitude of the applied voltage. In order to make the plasma response finite when the excitation frequency is in the vicinity of a normal mode frequency, collisional damping is included through the substitution of $\omega_p^2/\omega(\omega+i\nu) - 1$ for $\omega_p^2/\omega^2 - 1$, where ν is a collision frequency that is assumed small compared to ω. If we assume that ω is near a resonance ω_o of the fundamental k mode, i.e.,

$$ka\left(\frac{\omega_p^2}{\omega_o^2} - 1\right)^{1/2} \simeq \chi_{on}, \tag{47}$$

then we may separate the peak amplitude ϕ_p of this mode from Eq. (46) as

$$|\phi_p|^2 = \frac{16\ V_{rf}^2\ \omega_o^2}{\pi^2\ \chi_{on}^2\ J_1^2(\chi_{on})\ [(\omega - \omega_o)^2 + \nu^2/4]}, \tag{48}$$

in which ϕ_p is defined through

$$\tilde{\phi} = \phi_p\ J_o(\chi_{on}\ r/a)\ \sin kz. \tag{49}$$

This large amplitude wave produces a nonlinear density modification given by Eq. (43):

$$\delta n/n_o = \varepsilon(r)\ \cos 2kz, \tag{50}$$

with

$$\varepsilon(r) = \frac{k^2|\phi_p|^2\ \chi_{on}^2}{16\pi n_o m\omega_o^2 a^2}\ \left[\ J_1^2\ (\chi_{on}\ r/a) - (1 + 2k^2a^2)J_o^2(\chi_{on}\ r/a)\ \right] \tag{51}$$

Next we calculate the nonlinear modification to the Gould-Trivelpiece dispersion relation for small amplitude test waves supported by this modified plasma equilibrium. The partial differential equation for $\tilde{\phi}$, Eq. (15), when expressed in the strongly magnetized limit and with the time derivatives retained is

$$\frac{\partial^2}{\partial t^2}\ \nabla^2\ \phi + \frac{\partial}{\partial z}\left(\omega_p^2\ \frac{\partial}{\partial z}\ \phi\right) = 0. \tag{52}$$

The fractional density change $\delta n/n_o$ is included in Eq. (52) by substituting $\omega_p^2(1 + \delta n/n_o)$ for ω_p^2, giving

$$\frac{\partial^2}{\partial t^2}\ \nabla^2\ \phi\ + \omega_p^2\ \frac{\partial^2}{\partial z^2}\ \phi = -\omega_p^2\ \varepsilon(r)\ \frac{\partial}{\partial z}\left(\cos\ 2kz\ \frac{\partial}{\partial z}\ \phi\right). \tag{53}$$

Equation (53) is solved for the eigenmodes of the modified system when $\delta n/n_o << 1$ by a perturbation technique in which the solutions are expanded in terms of the solutions of the equation with $\varepsilon = 0$. Assuming that the solution consists of a perturbation to a small amplitude test wave of the form

$$\phi = f(z,t)\, J_\ell(\chi_{\ell m}\, r/a)\, \exp(i\ell\theta), \tag{54}$$

in which

$$f(z,t) = \phi_+ \exp[i(k_j z - \omega_j t - \delta\omega_j t)] + \phi_- \exp[i(-k_j z - \omega_j t - \delta\omega_j t)], \tag{55}$$

and k_j and ω_j are related through the dispersion relation for the unperturbed system,

$$k_j^2 a^2 = -\frac{\chi_{\ell m}^2}{1 - \omega_p^2/\omega_j^2}\,. \tag{56}$$

The $\varepsilon(r)$ term causes the frequency shift $\delta\omega_j$ appearing in Eq. (55) and introduces additional radial and axial modes with frequencies other than ω. In this study we do not consider these additional modes; instead we concentrate on the frequency shift $\delta\omega_j$.

Inserting Eqs. (54) and (55) into Eq. (53), multiplying by $rJ_\ell(\chi_{\ell m}\, r/a)\exp(-i\ell\theta)$, integrating in r from 0 to a, and projecting out the z independent component gives

$$(\delta\omega_j/\omega_j)\, a^2\, J_{\ell+1}^2(\chi_{\ell m})\left(|\phi_+|^2 + |\phi_-|^2\right) = -\left(\phi_-^*\,\phi_+ + \phi_-\phi_+^*\right)\int_o^a rdr\ \varepsilon(r)\ J_\ell^2(\chi_{\ell m}\, r/a). \tag{57}$$

The $\varepsilon(r)$ term introduces a coupling between the right going and left going waves when $k_j = k$. The physical reason is as follows: The density ripple has an axial wavenumber of 2k while the difference in wavenumber between left traveling and right traveling waves is $2k_j$. Thus when $k = k_j$ the density ripple couples the left traveling and right traveling waves.

Specializing to an axially standing wave with $\phi_+ = \phi_j/2i$, $\phi_- = -\phi_j/2i$, and $k = k_j$, Eq. (57) becomes

$$\delta\omega_j/\omega_j = \left(\int_o^a r\,dr\ \varepsilon(r)\ J_\ell^2(\chi_{\ell m}\ r/a)\right)\left(a^2\ J_{\ell+1}^2\ (\chi_{\ell m})\right)^{-1}, \tag{58}$$

and ϕ_j is a constant amplitude of the small amplitude test wave. Substituting Eq. (51) into Eq. (58) gives

$$\delta\omega_j/\omega_j = \frac{-\ k^2|\phi_p|^2}{16\pi a^2 n_o m\omega_o^2 J_{\ell+1}^2(\chi_{\ell m})}\ [(\chi_{on}^2 + 2k^2a^2)\ C - \chi_{on}^2\ D], \tag{59}$$

where

$$C \equiv \int_0^1 u\,du\ J_\ell^2(\chi_{\ell m}\ u)\ J_o^2(\chi_{on}\ u),$$

$$D \equiv \int_0^1 u\,du\ J_\ell^2(\chi_{\ell m}\ u)\ J_1^2(\chi_{on}\ u). \tag{60}$$

Since Eq. (59) describes the nonlinear frequency shift of axially standing small amplitude test waves (of linear frequency ω_j) due to the presence of the large amplitude axisymmetric standing wave at frequency ω_o, we require that either $m \neq n$ or $\ell \neq 0$. This frequency shift is nonzero only when the test wave has the same axial dependence of sinkz as the large amplitude wave.

The previous analysis also describes the self-modification of the large amplitude mode. If $m = n$ and $\ell = 0$ then ω_j becomes ω_o, $\delta\omega_j$ becomes $\delta\omega_o$, ϕ_j becomes ϕ_p, and Eq. (59) describes the nonlinear frequency shift of the large amplitude mode:

$$\delta\omega_o/\omega_o = \frac{-\ k^2|\phi_p|^2}{18\pi a^2 n_o m\omega_o^2 J_1^2(\chi_{on})}\left[\chi_{on}^2\ E + k^2a^2\ F\right], \tag{61}$$

where

$$E \equiv \int_0^1 u\,du\; J_o^2(\chi_{on}\, u)\; J_1^2(\chi_{on}\, u),$$

$$F \equiv \int_0^1 u\,du\; J_o^4(\chi_{on}\, u). \tag{62}$$

Replacing ω_o in the resonant denominator of Eq. (48) with $\omega_o + \delta\omega_o$, using Eq. (61) for $\delta\omega_o$, and defining the scaling parameters,

$$\phi_s \equiv \frac{8\omega_o V_{rf}}{\pi\nu\chi_{on} J_1(\chi_{on})}, \tag{63}$$

$$p \equiv \frac{8k^2\omega_o V_{rf}^2}{\pi^3 a^2 n_o m\nu^3 \chi_o^2 J_1^2(\chi_{on})}\,[\chi_{on}^2\, E + k^2 a^2\, F], \tag{64}$$

$$\Delta\omega \equiv \omega - \omega_o, \tag{65}$$

gives a nonlinear equation for the wave amplitude,

$$|\phi_p/\phi_s|^2 = \frac{1}{[2\Delta\omega/\nu + 2p|\phi_p/\phi_s|^2]^2 + 1}\,. \tag{66}$$

The resulting scaled wave amplitude ϕ_p/ϕ_s obtained by numerical solution of Eq. (66) is plotted in Fig. 7 for several values of the nonlinearity parameter p. For values of $p \gtrsim 1$ the plots of wave amplitude become multiple-valued. Since only one value is physically possible, this causes the system to follow different amplitude versus frequency curves depending upon the direction the excitation frequency is swept through the resonance frequency. Figure 8 shows this hysteresis effect for p = 2. If the frequency ω is swept slowly up (i.e., increased) through resonance compared to the system relaxation time $1/\nu$, the system response follows the curve from A to C, jumps up to point E, and continues along the curve to F. When

the frequency is swept down slowly, the system response follows the path FDBA. An analogous hysteresis effect has recently been experimentally observed[7] in a two-dimensional nonneutral plasma consisting of charges suspended below the surface of liquid helium.

V. Conclusions

The present analytical study illustrates the principal features of the ponderomotive effect in nonneutral plasmas. Whereas in a neutral plasma the ponderomotive force is balanced against plasma pressure, in a nonneutral plasma it is balanced against self-consistent space charge fields. The consequence of self-consistency in a finite geometry is that the local density change produced by the ponderomotive force is not simply related to the local strength of the electric field amplitude, as is the case for a neutral plasma. Consequently, the usual formula $\delta n/n_o = - |\underset{\sim}{E}|^2/16\pi n_o T$, does not hold in the nonneutral system. Instead, the global properties of the system are important. This leads to a situation in which near the axis of the nonneutral column a density change given approximately by $\delta n/n_o = -(\chi_{on}^2/a^2)\ \delta|\tilde{E}_z|^2/8\pi n_o m\omega^2$, in which $-\chi_{on}^2/a^2$ is the radial curvature of $|\tilde{E}_z|^2$ on the axis. At outer radii the radial curvature of $|\tilde{E}_z|^2$ becomes positive, and a reversal in sign of the density change results. This effect is associated with the fringing of the space charge field, as discussed in Sec. III.

In addition to the density changes, the ponderomotive force is found to alter the zero order rotation of the nonneutral plasma column. In particular it introduces a velocity shear whose consequences have not been explored in this study.

To obtain concrete results which are manageable analytically, the present study has examined in detail the ponderomotive changes produced by an ideal large amplitude standing Gould-Trivelpiece mode. For simplicity, the plasma is taken to be infinite in axial extent. While this model is necessarily restricted, the results obtained are expected to be characteristic of these systems. However, the usage of more realistic waveforms and consideration of finite axial

extent should yield more accurate results that may fit closer the actual experimental situation. The additional anticipated effect not included in the present model is an axial elongation of a finite length column.

This study has also evaluated the lowest order consequences of the nonlinear changes in density produced by the ponderomotive force. It is found that the linear dispersion relation is modified, and results in a frequency shift for some of the standing waves in the system which satisfy the appropriate matching conditions explained in Sec. IV. The result is evaluated for additional test waves as well as for the large amplitude wave responsible for the density rearrangement. In this latter case, an interesting hysteris effect is obtained. It arises because the resonant response function (i.e., the usual Lorentzian line) becomes amplitude dependent. Consequently, when the nonlinear frequency shift becomes comparable to the collisional broadening of the resonance, an asymmetry in the response results. As the external driving frequency is swept slowly, different amplitudes can be generated which correspond to the various solutions of a cubic equation. An analogous effect has been recently observed in an experiment[7] involving a two dimensional nonneutral plasma generated by attaching charges below the surface of liquid Helium. The present results indicate that a similar effect should also occur in a 3-dimensional nonneutral plasma.

Finally, the feasibility of experimental observation of the effects predicted is assessed. Considering a presently attainable peak electron density[5] $n_p = 1.3 \times 10^7$ cm^{-3} ($\omega_p = 2 \times 10^8$ rad/sec) and column radius a = 2 cm, one finds a relation between the peak potential amplitude ϕ_p for the standing wave, taken as the lowest radial Gould-Trivelpiece mode, and the fractional density $\delta n/n_o$, $\phi_p \simeq 45(\delta n/n_o)^{1/2}$ volts. The self-consistent ϕ_p can be related to the external

potential V_{RF} through the Q of the mode, i.e., $\phi_p \simeq 2QV_{RF}$. For a $Q \simeq 100$, an external excitation of the order of 22 mV is predicted to result in a 1% density change, which should be measurable. Concerning the distortion of the resonant curve due the nonlinear frequency shift, it should be noted that interesting effects begin to appear when the nonlinear parameter p, defined in Eq. (65), is of order unity. The condition $p = 1$ requires an external excitation $V_{RF} \simeq 70\ Q^{-3/2}$ volts which again, for a $Q \simeq 100$, predicts $V_{RF} \simeq 70$ mV, thus suggesting that the effect should be amenable to experimental investigation.

Acknowledgments

The authors are grateful for discussions with Professor G. A. Williams concerning his liquid helium experiment. We also acknowledge useful discussions with Dr. D. L. Eggleston regarding the feasibility of an experimental test of our results.

The contents of this paper form a portion of the dissertation submitted by one of the authors (B. M. L.) in partial fulfillment of the requirements leading to the Ph.D. degree.

This work was supported by the Office of Naval Research.

References

1. H. Motz and C. J. H. Watson, Advances in Electronics and Electron Physics 23, 1534 (1967).
2. J. R. Cary and A. N. Kaufman, Phys. Fluids 24, 1238 (1981).
3. A. W. Trivelpiece and R. W. Gould, J. Appl. Phys. 30, 1784 (1959).
4. S. A. Prasad and T. M. O'Neil, Phys. Fluids 26, 665 (1983).
5. J. H. Malmberg and J. S. deGrassie, Phys. Rev. Lett. 35, 577 (1975).
6. G. Dimonte, Phys. Rev. Lett. 46, 26 (1981).
7. M. L. Ott-Rowland, V. Kotsubo, J. Theobald, and G. A. Williams, Phys. Rev. Lett. 49, 1708 (1982).
8. R. C. Davidson and N. A. Krall, Phys. Fluids 13, 1543 (1970).
9. B. L. Bogema, Jr. and R. C. Davidson, Phys. Fluids 13, 2772 (1970).
10. S. A. Prasad and T. M. O'Neil, Phys. Fluids 22, 278 (1979).
11. T. M. O'Neil and C. F. Driscoll, Phys. Fluids 22, 266 (1979).

FIGURE CAPTIONS

Fig. 1 a) Schematic of geometry and large amplitude $\ell = 0$ axially standing wave. b) Typical zero order density profile for $a = 10\ \lambda_D$ and radial dependence of the lowest order Gould-Trivelpiece mode.

Fig. 2 Radial dependence of $\delta|\tilde{E}_z|^2$ for the lowest order radial mode, evaluated at the axial position $z = 0$. The axial dependence is cos2kz.

Fig. 3 Radial dependence of the nonlinear density rearrangement $\delta n/n_s$, due to the mode in Fig. 2, evaluated at the axial position $z = 0$. The axial dependence is cos2kz. δn is shown for three different plasma temperatures in the limit $ka << 1$.

Fig. 4 Schematic of the plasma response to the ponderomotive force of a standing wave showing the fringing electrostatic field lines for a positive ion plasma. The physical interpretation follows Eq. (43).

Fig. 5 Radial dependence of δV_θ evaluated at the axial position $z = 0$. The axial dependence is cos2kz.

Fig. 6 An idealized antenna for exciting standing waves.

Fig. 7 Scaled wave amplitude ϕ_p/ϕ_s versus excitation frequency ω for three values of the nonlinear parameter p.

Fig. 8 Scaled wave amplitude ϕ_p/ϕ_s versus excitation frequency ω for $p = 2$. When frequency is swept up (i.e., increased) the wave amplitude follows ACEF. When frequency is swept down (i.e., decreased) the wave amplitude follows FDBA.

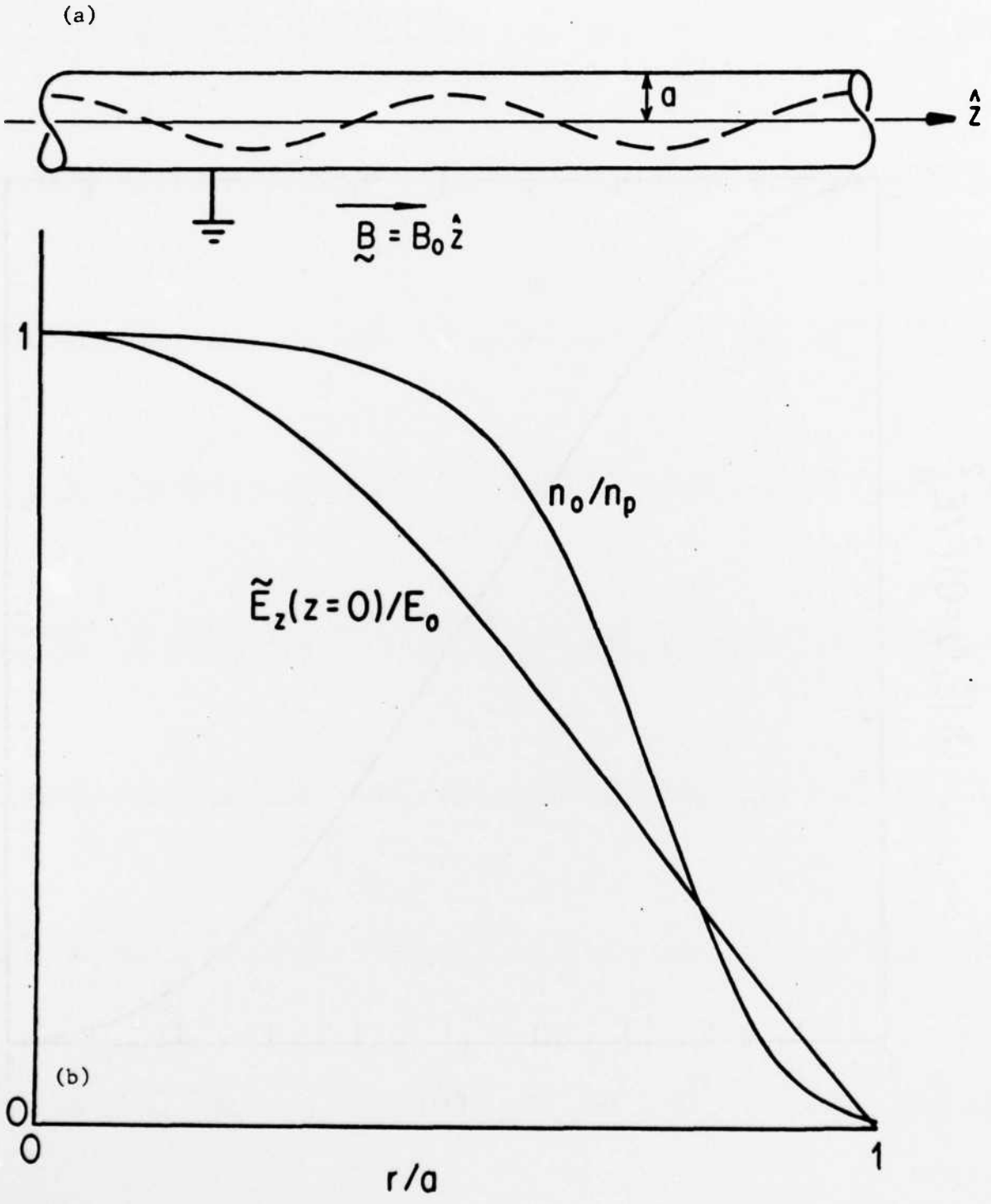

Fig. 1

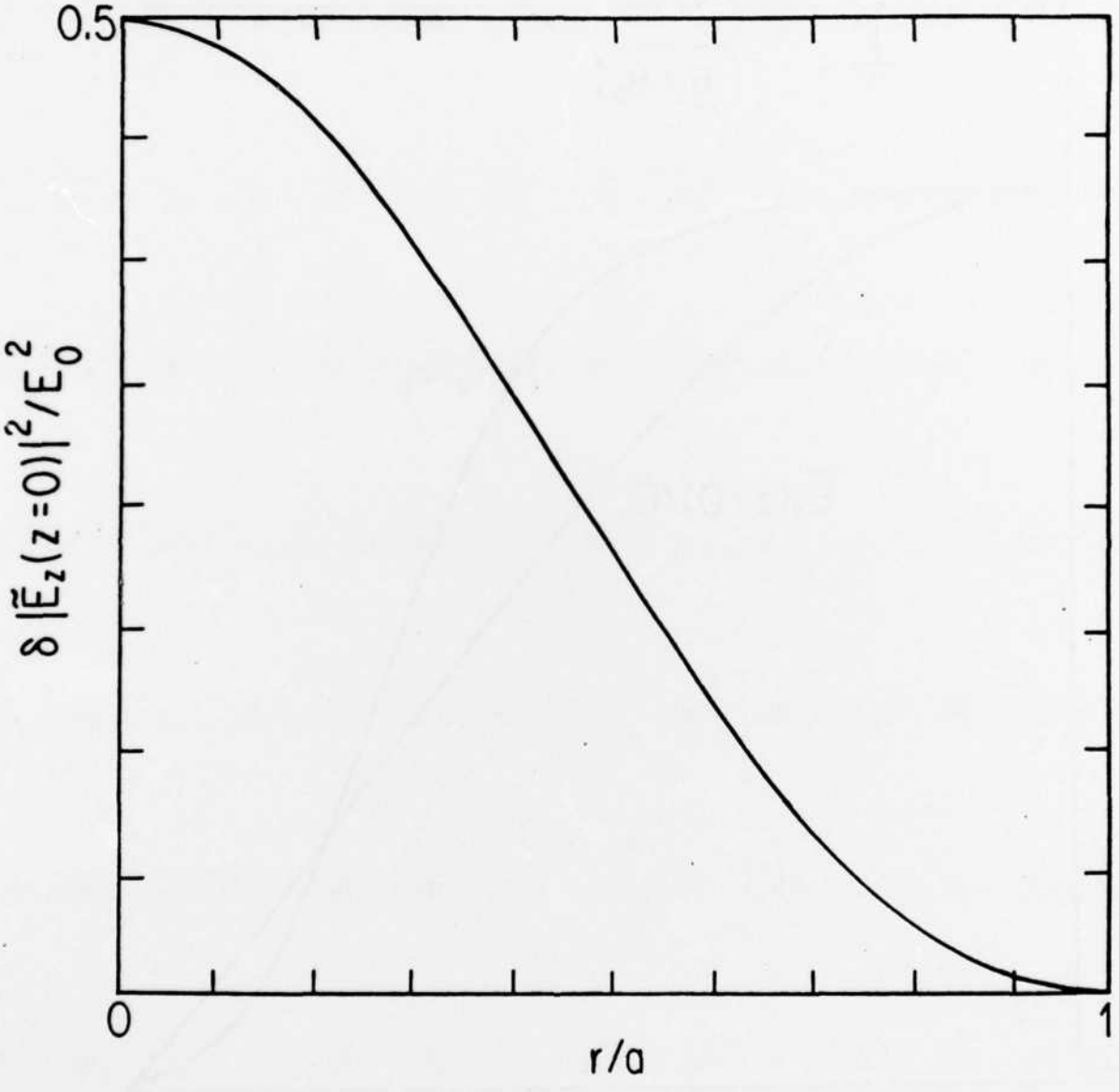

Fig. 2

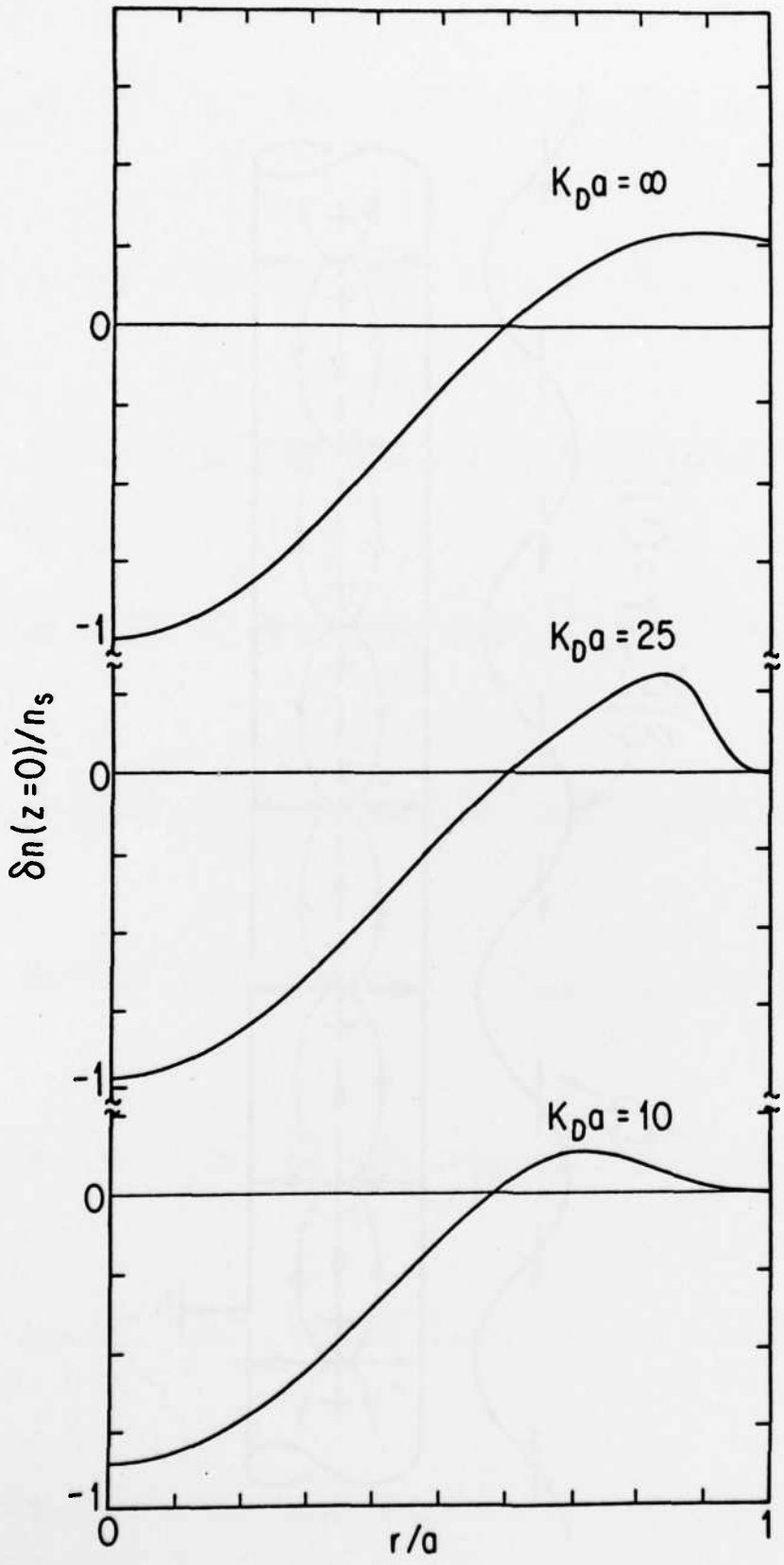

Fig. 3

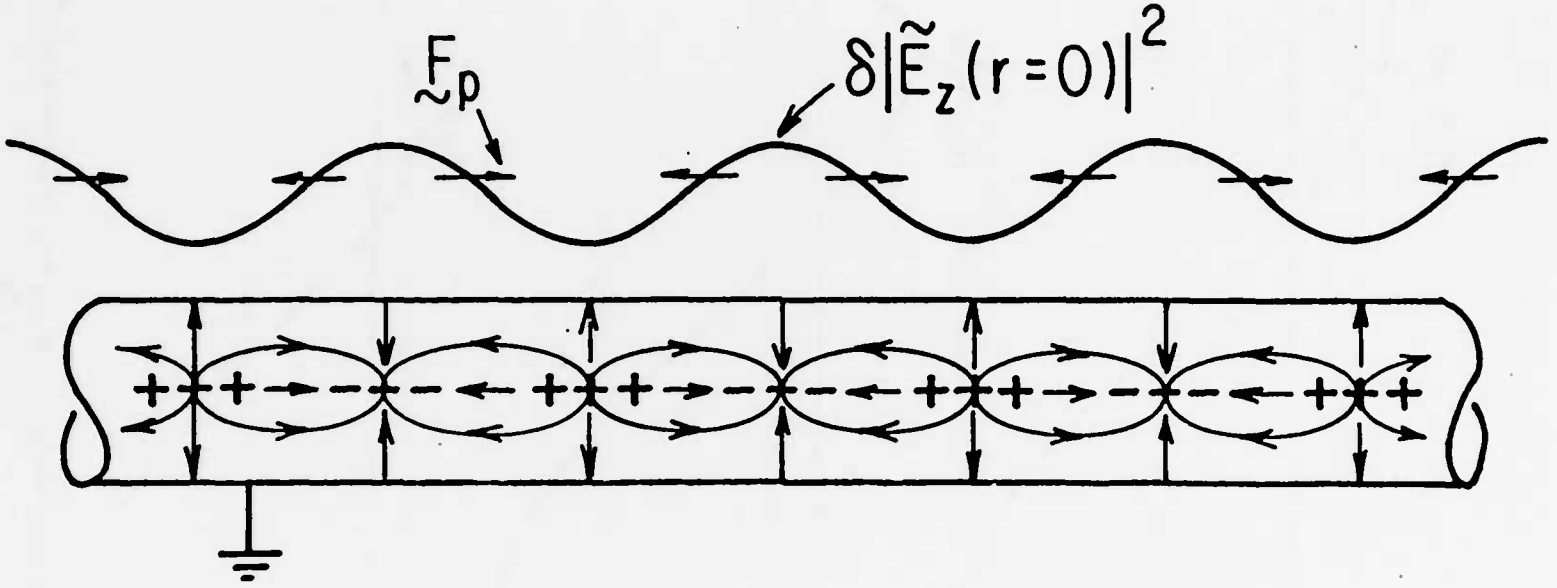

Fig. 4

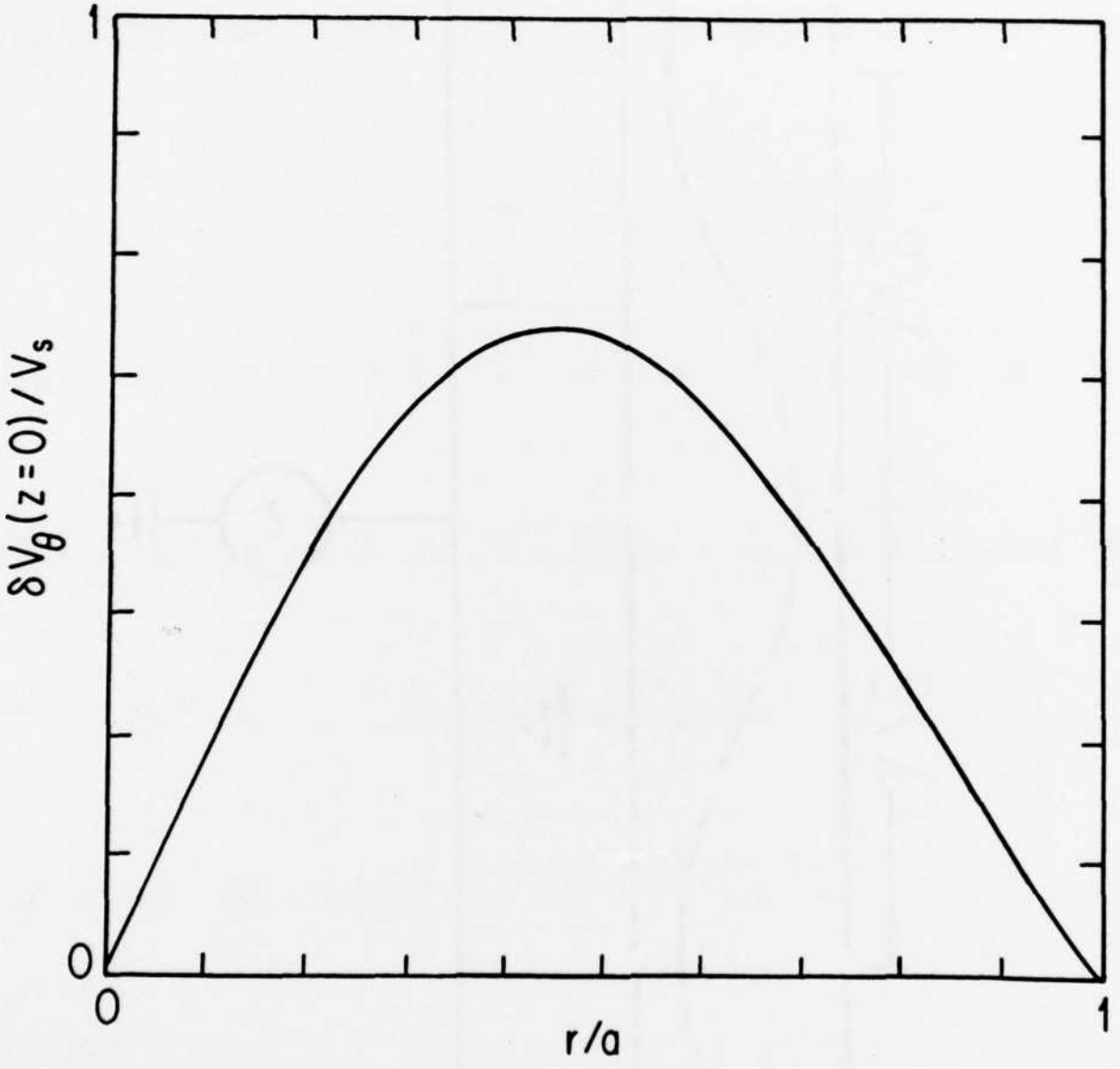

Fig. 5

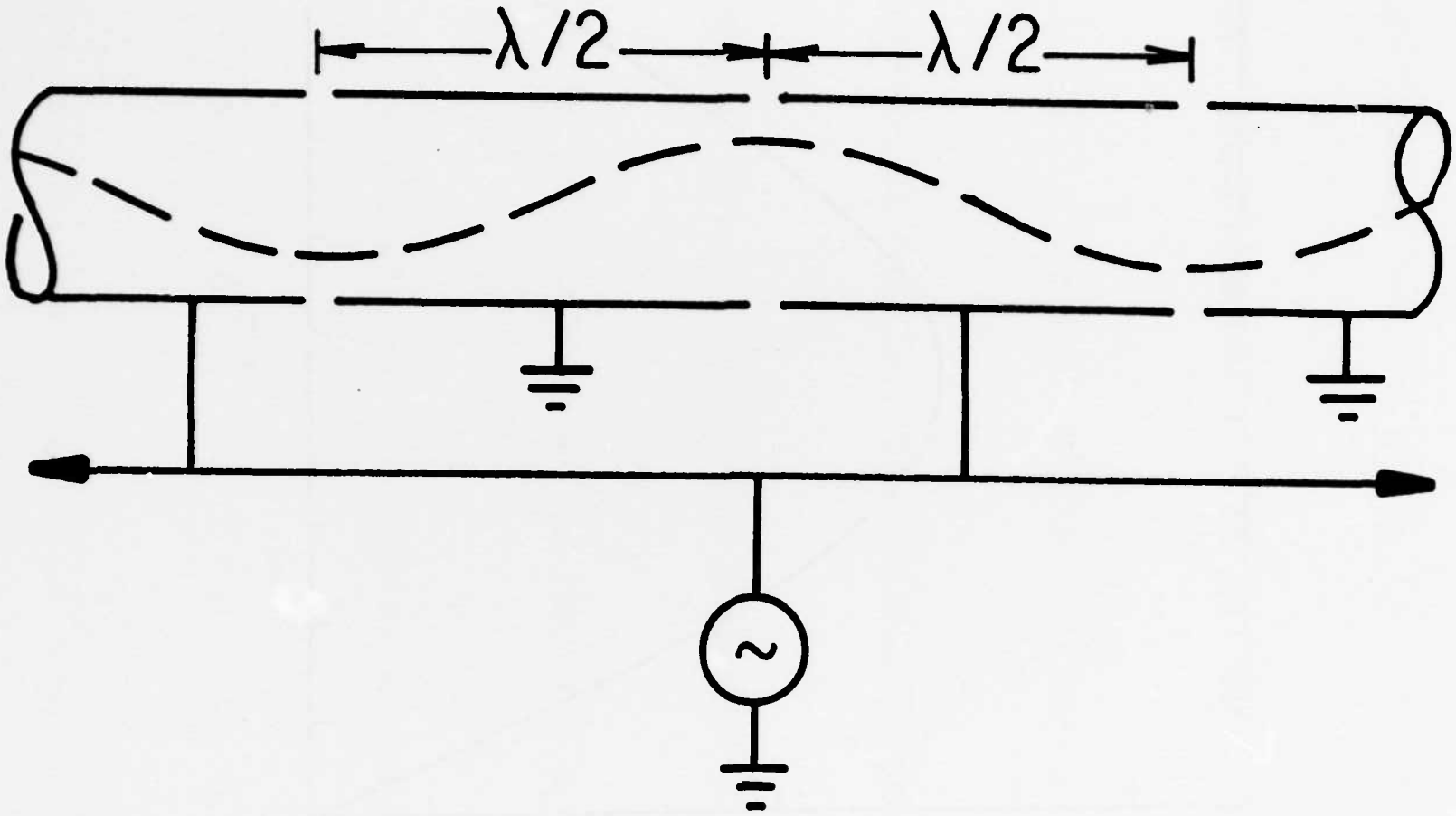

Fig. 6

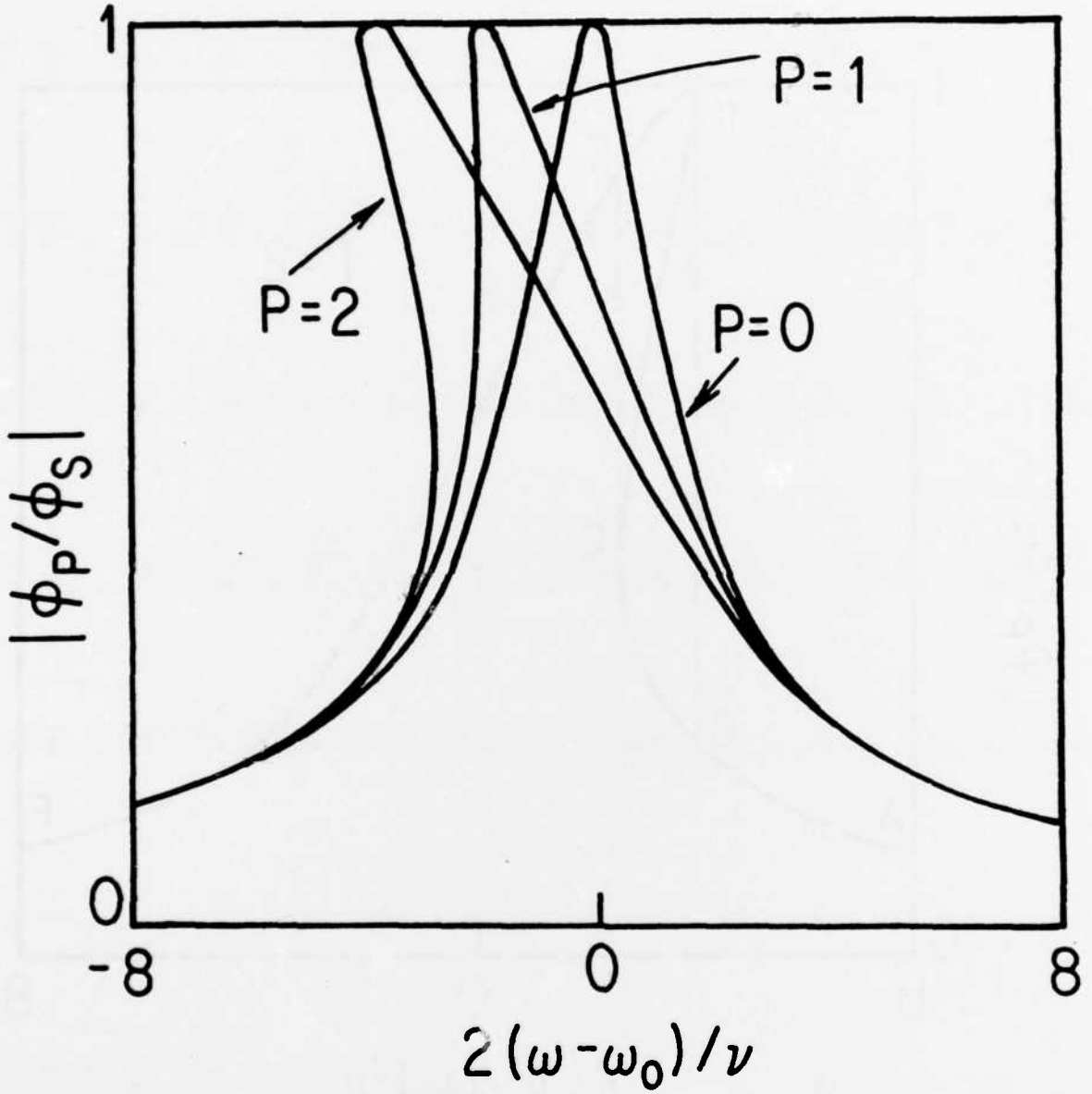

Fig. 7

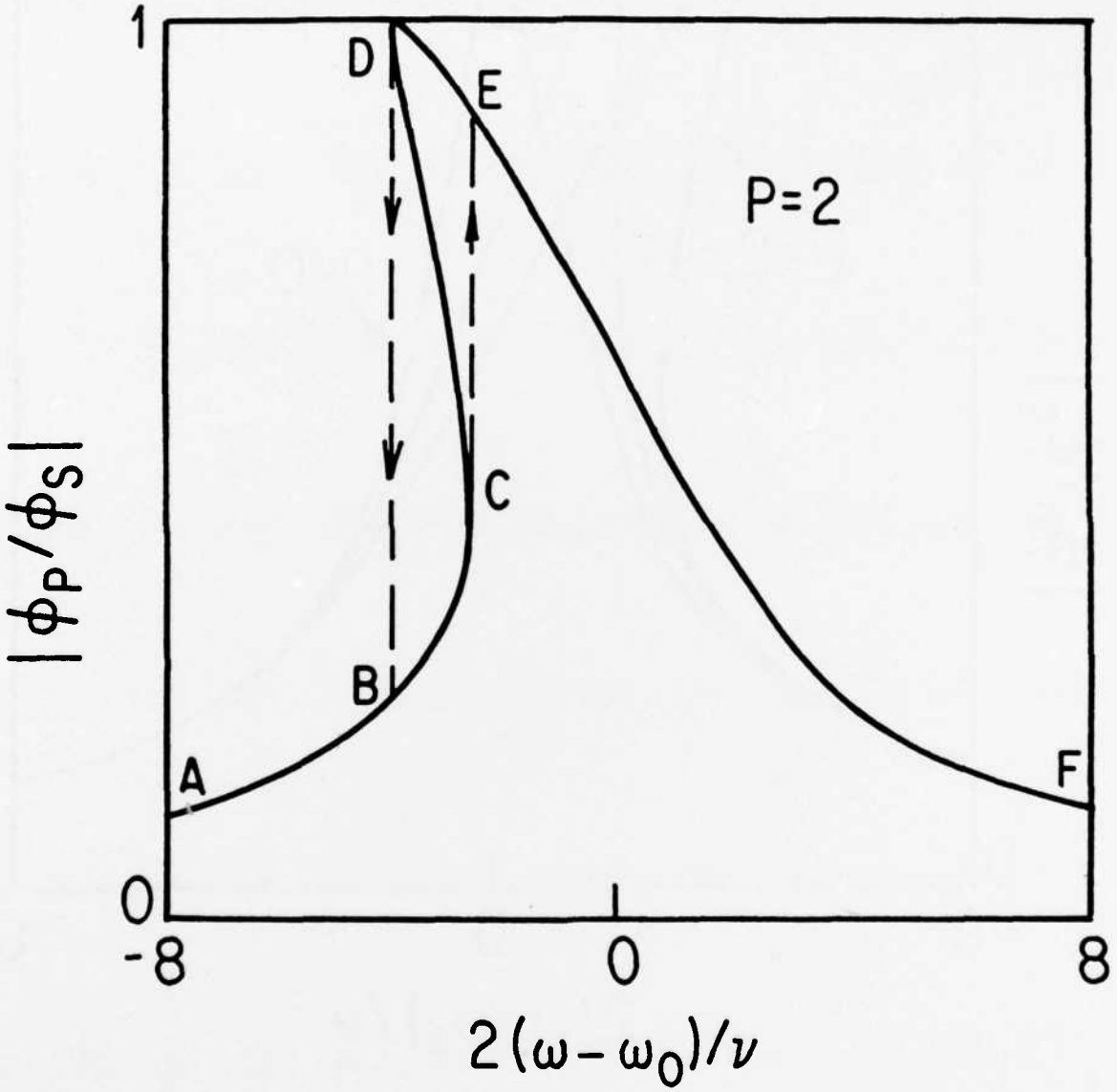

Fig. 8

PPG-673 "On the Origin of Plasmospheric Hiss: Ray Path Integrated Amplification," S. R. Church, R. M. Thorne, submitted to Journal of Geophysical Research, December, 1982

PPG-674 "High Frequency Instabilities in Underdense Plasmas Produced by 0.35 micrometer Laser Beam," H. Figueroa, C. Joshi, C. E. Clayton, H. Azechi, N. A. Abraham, K. Estabrook, December, 1982.

PPG-675 "Magnetic Field Line Reconnection Experiments--Part 5: Current Disruptions and Double Layers", R. L. Stenzel, W. Gekelman, and N. Wild, December, 1982

PPG-676 "Relativistic Magnetohydrodynamic Winds of Finite Temperature," C. F. Kennel, F. S. Fujimura, and I. Okamoto, 1983.

PPG-677 "Magnetohydrodynamic Model of Crab Nebula Radiation," C. F. Kennel and F. V. Coroniti, 1983.

PPG-678 "Cascade-Diffusion Theory Including Cascade Size Effects," P. Chou, N. M. Ghoniem, S. Sharafat, January, 1983.

PPG-679 "The Dependence of the Drift Cyclotron Loss Cone Instability on the Radial Density Gradient," J. Ferron, A. Wong, and B. Leikind, January, 1983, submitted to Phys. Fluids.

PPG-680 "Interchange Stability of an Axisymmetric, Average MInimum B Magnetic Mirror" by J. Ferron, A. Wong, G. Dimonte B. Leikind, being submitted Physics of Fluids, January, 1983.

PPG-681 "Experimental Modelling of Satellite Wakes in Auroral Arcs" by N. Wild, R. L. Stenzel & W. Gekelman submitted to Geophys. Rev. Lett., January 1983

PPG-682 "Nonlinear Energy Flow in a Beam Plasma System," by D. A. Whelan & R. L. Stenzel, submitted to Phys. Rev. Letts February, 1983

PPG-683 "Ion Heating and Acceleration by Strong Magnetosonic Waves" by B. Lembege, S. T. Ratliff, J. M. Dawson, Y. Ohsawa, submitted to the Physical Rev. Lett., February, 1983

PPG-684 "Global in Elastic Structural Analysis of the MARS Tandem Mirror Blanket Tubes Including Radiation Effects," J. P. Blanchard & N. Ghoniem, February (1983).

PPG-685 "Cyclotron Resonance RF Acceleration in a TE_{111} Cavity," D. B. McDermott, N. C. Luhmann, Jr., and D. S. Fururo, February (1983).

PPG-686 "Operation of a Milimeter-Wave Harmonic Gyrotron," D. B. McDermott, N . C. Luhmann, Jr., D. S. Fururo, A. Kupiszewski, February, (1983).

PPG-687 "Electromagnetic Ion Cyclotron Instability in the Multi-ion Jovian Magnetosphere", R. M. Thorne, J. J. Moses, submitted to Journal of Geophysical Research Letters, March, 1983

PPG-688 "Observations of Odd-Half Cyclotron Harmonic Emissions in a Shell-Maxwellian Laboratory Plasma," J. M. Urrutia and R. L. Stenzel, March, 1983. To be submitted to JGR.

PPG-689 "Plasma Parameters, Fluctuations and Kinetics in a Magnetic Field Line Reconnection Experiment," N. Wild, March, 1983.

PPG-690 "A Plasma Wave Accelerator - Surfatron I and II," T. Katsouleas, J. M. Dawson, W. Mori, and C. Joshi, March, 1983/

PPG-691 "Electromagnetic Radiation and Nonlinear Energy Flow in a Beam Plasma System," David A. Whelan, March (1983)

PPG-692 "The Surfatron Laser-Plasma Accelerator", T. Katsouleas and J. M. Dawson, submitted to Phys. Rev. Lett. April, 1983

PPG-693 "The Reactor Physics of Startup Shutdown and Staged Power Operation in Tandem Mirror Reactors," R. Conn, F. Najmabadi, F. Kantrowitz, M. Firestone, D. Goebel, and T.K. Mau, April (1983).

PPG-694 "Transport and Ray Tracing Studies of ICRF-Heated Tokamak Reactors," T. K. Mau and R. W. Conn, April (1983).

PPG-695 "Directional Velocity Analyzer for Measuring Eelctron Distribution Functions in Plasmas", R. Stenzel, W. Gekelman, N. Wild, M. Urrutia and D. Whelan, April, 1983.

PPG-696 "Shape of the Magnetosphere", C. C. Wu, accepted for publication Geophys. Res. Lett., April, 1983

PPG-697 "Anomalous Transport by Magnetohydrodynamic Kelvin-Helmholtz Instabilities in the Solar Wind-Magnetosphere Interaction", A. Miura, submitted to Jour. Geo. Res., April 1983

PPG-698 "Helium Effects on Solids - a Reference Manual", N. Ghoniem and P. Maziasz, April 1983.

PPG-699 "Global Inelastic Structural Analysis of the Mars Tandem Mirror Blanket Tubes Including Radiation Effects", J. P. Blanchard and N. Ghoniem, April 1983.

PPG-700 "Self-Modulation Formation of Pulsar Microstructures" by A.C.-L. Chian and C. F. Kennel, to be submitted to Astrophysics and Space Science, May 1983.

PPG-701 "Evolution from Coherence to Turbulence in Plasmas," A. Y. Wong, P. Cheung, and T. Tanikawa, submitted to Proceedings in Inter-science Series on Statistical Physics, May 1983.

PPG-702 "Trapping of Plasma Waves in Cavitons", T. Tanikawa, A. Y. Wong and D. L. Eggleston, submitted to Phys. Fluids, May 1983.

PPG-703 "Instrumentation for Magnetically Confined Fusion Plasma Diagnostics", N.C. Luhmann Jr. and W. A. Peebles, invited review for Review of Scientific Instruments, May 1983.

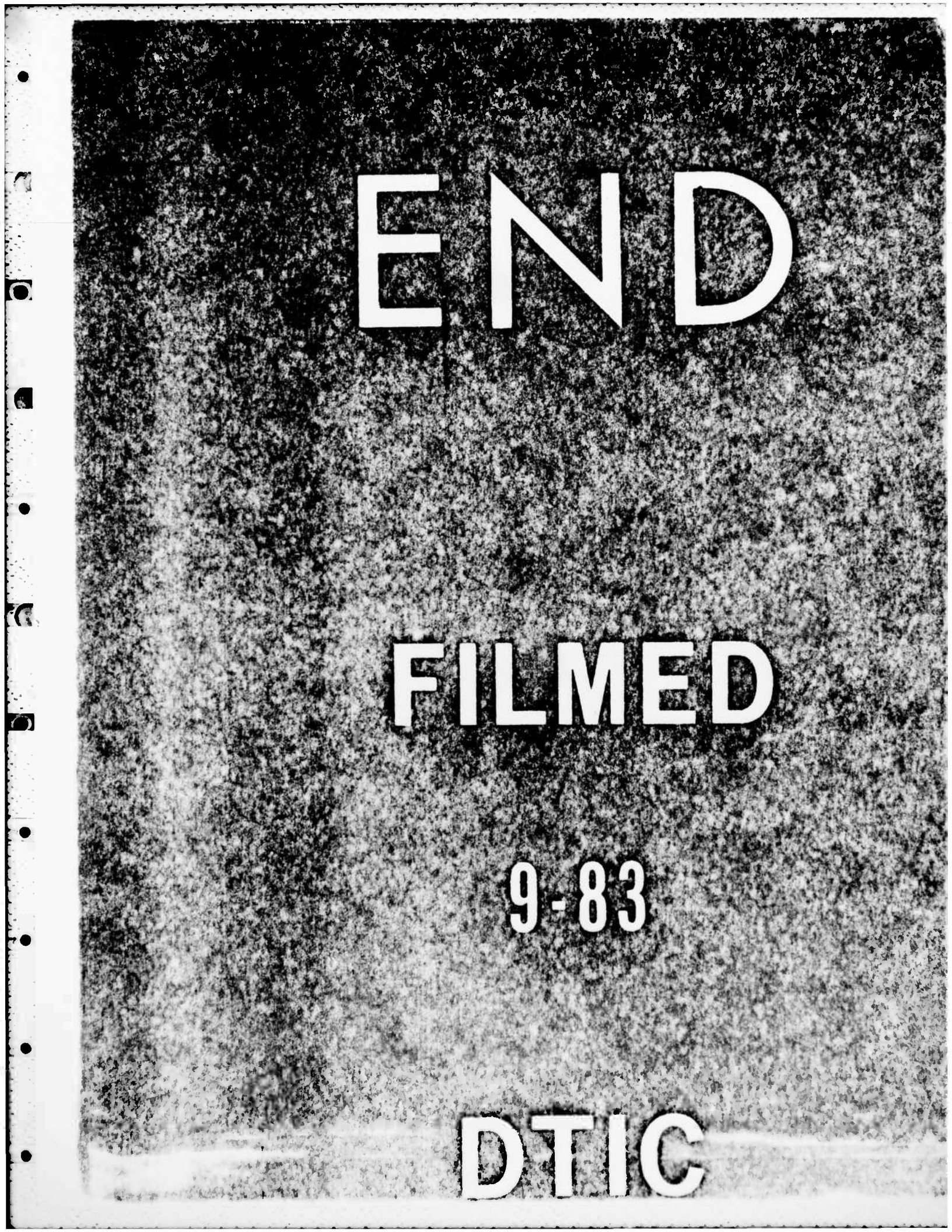
END
FILMED
9-83
DTIC